^{15}N NMR and Electrochemical Studies of [Ru^{II}(hedta)]$^{-}$ Complexes of NO, NO^{+}, NO$_2$$^{-}$, and NO^{-}

Ya Chen, Fu-Tyan Lin, and Rex E. Shepherd*

Department of Chemistry, University of Pittsburgh, Pittsburgh, Pennsylvania 15260

Received July 23, 1998

[Ru^{II}(hedta)L]$^{n-}$ complexes (hedta^{3-} = *N*-(hydroxyethyl)ethylenediaminetriacetate; L = NO^{+}, n = 0; L = NO, n = 1; L = NO^{-}, n = 2) have been prepared by the displacement of H$_2$O/D$_2$O via NO(g) or NO$_2$$^{-}$. This is the first reported entire set of NO^{+}, NO, and NO^{-} as ligands for the same metal center in a constant oxidation state and with a constant ligand environment (here Ru^{II} and the amino carboxylate hedta^{3-}). From the NO stretching frequencies of isolated salts, the net influence of back-donation by Ru^{II} and its σ-withdrawal was observed to be that the bond order for the NO^{+} complex is virtually the same (ca. 2.46) as that for the NO complex (ca. 2.48). The back-donation to NO^{-} is also small, as is that to NO, but orbital mixing of NO^{-} and Ru^{II} is sufficiently important to induce a singlet NO^{-} complex. Values for the ν_{NO} in cm^{-1} for the ^{14}N- and ^{15}N-labeled complexes, respectively, are as follows: NO^{+}, 1846, 1827; NO, 1858, 1842; NO^{-}, 1383, 1370. Combined results of ^{15}N, ^{13}C, and ^{1}H NMR spectra of the complexes in D$_2$O show that [Ru^{II}(hedta)(^{15}NO^{+})] is a single cis-equatorial isomer with its ^{15}NO^{+} resonance at 249.6 ppm vs [^{15}N]formamide. The two-electron-reduced [Ru^{II}(hedta)(^{15}NO^{-})]$^{2-}$ complex exists as trans- and cis-equatorial isomers having ^{15}NO^{-} resonances at 609.4 and 607.4 ppm. The ^{15}N resonances appear at 260.0 ppm for the ^{15}NO^{+} ligand and at 348.8 ppm for the bound ^{15}NO$_2$$^{-}$ ligand in the [Ru^{II}(hedta)(^{15}NO$_2$$^{-}$)(^{15}NO^{+})(D$_2$O)] complex. Differential pulse voltammetric waves for the [Ru^{II}(hedta)L]$^{n-}$ series occur at −0.37 V for the Ru^{II}(NO^{-})/Ru^{II}(NO) couple, at −0.10 V for the Ru^{II}(NO)/Ru^{II}(NO^{+}) couple, and at +0.98 V for the Ru^{II}(NO^{+})/Ru^{III}(NO^{+}) couple. The coordinated nitrosyl ion/nitro equilibrium (L′)Ru^{II}(NO^{+}) + 2OH^{-} ⇌ (L′)Ru^{II}(NO$_2$$^{-}$) + H$_2$O ($K_{NO_2^-}$) was observed for L′ = hedta^{3-}, as for previous examples with L′ = violurate, polypyridyl ligands, and (CN^{-})$_5$ and (NH$_3$)$_5$ ligand sets. $K_{NO_2^-}$ = 1.44 × 10^{13} for L′ = hedta^{3-}. log-($K_{NO_2^-}$) is linearly related through the ion-pairing equilibrium constant expression to −z_1z_2, the charge product of the reacting ions (here the (L′)Ru(NO^{+}) complex and OH^{-}) from −4 through +3, excluding the (NH$_3$)$_m$ ammine series with m = 4 and 5. The opposite behavior of the ammines is attributed to strong solvent H-bonding that changes for reactant and product in the nitrosyl/nitro equilibrium. The pK_a of coordinated nitrous acid in [Ru^{II}(hedta)(HONO)]$^{-}$ is calculated to be −0.80, a 3.85 log unit enhancement over free HONO due to the Ru^{II} charge. An MO explanation is presented to interrelate the {Fe^{III}−(NO^{-} triplet)} complexes, the {Ru^{II}−(NO^{-} singlet)} type observed for [Ru^{II}(hedta)(^{15}NO^{-})]$^{2-}$, and the NO^{+} complexes of other strong-field metals. When both d$_{z^2}$ and d$_{x^2-y^2}$ metal orbitals reside below the NO π* pair, the electronic repulsions favor a bent NO^{-} triplet ligand. If both metal orbitals reside above the NO π* pair, the orbital mixing and back-donation induce a coordinated NO^{-} singlet ligand, and if the NO π* pair reside between the two σ-based d orbitals, an NO^{+} ligand and reduced metal center obtain.

Introduction

The interest in ruthenium nitrosyl complexes has been rekindled by recent discoveries of uses for ruthenium nitrosyls as antitumor and antisepsis agents.[1−4] Throughout the past quarter-century there has been a continuing interest in the various redox assignments as NO^{+}, NO•, or NO^{-} [8−11] that should be given to NO-coordinated species.[5−14] An early issue

was whether a bent NO complex might be properly termed an NO^{-} complex. The question of the existence of coordinated NO^{-} was answered by the crystal structure of [IrCl(PPh$_3$)$_2$(CO)-(NO)][BF$_4$], which required an NO^{-} ligand to account for the
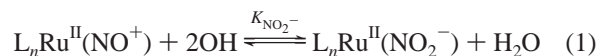
(1) Fricker, S. P.; Slade, E.; Powell, N. A.; Vaughn, O. J.; Henderson, G. R.; Murrer, S. A.; Megson, I. C.; Bisland, S. K.; Flitney, F. W. *Br. J. Pharmacol.* **1997,** *122,* 1441.

(2) Bettache, N.; Carter, T.; Corrie, J. E. T.; Ogden, D.; Trentham, D. R. In *Methods in Enzymology*; Packer, L., Ed.; Academic Press: San Diego, CA 1996; Vol. 268, pp 266−281.

(3) Davies, N.; Wilson, M. T.; Slade, E.; Fricker, S. P.; Murrer, B. A.; Powell, N. A.; Henderson, G. R. *J. Chem. Soc., Chem. Commun.* **1997,** 47.

(4) Chen, Y.; Shepherd, R. E. *J. Inorg. Biochem.* **1997,** *68,* 183.

(5) Enemark, J. H.; Feltham, R. D. *Coord. Chem. Rev.* **1994,** *13,* 339.

(6) McCleverty, J. *Chem. Rev.* **1979,** *79,* 53.

(7) Richter-Addo, G. B.; Leggdins, P. *Metal Nitrosyls*; Oxford University Press: New York, 1992.

(8) Livingstone, S. E. In *Comprehensive Inorganic Chemistry*; Pergamon: Oxford, U.K., 1973; p 1200.

(9) Stamler, J. S.; Surjel, D. J.; Loscalzo, J. *Science* **1992,** *258,* 1898.

(10) Enemark, J. H.; Feltham, R. D. *Proc. Natl. Acad. Sci. U.S.A.* **1972,** *69,* 3534.

(11) (a) Johnson, B. F. G.; Haymore, B. L.; Dilworth, J. R. In *Comprehensive Coordination Chemistry*; Wilkinson, G., Gillard, R. D., McCleverty, J., Eds.; Pergamon: New York, 1987; Vol. 2, pp 100−107. (b) Collman, U. P.; Hoffman, N. W.; Morris, D. E. *J. Am. Chem. Soc.* **1969,** *91,* 5659. (c) Basolo, F.; Pearson, R. G. *Mechanisms of Inorganic Reactions*; Wiley: New York, 1967; p 573.

(12) (a) Hodgson, D. J.; Payne, N. C.; McGinnety, J. A.; Pearson, R. G.; Ibers, J. A. *J. Am. Chem. Soc.* **1968,** *90,* 4486. (b) Hodgson, D. J.; Ibers, J. A. *Inorg. Chem.* **1968,** *7,* 2345.

(13) Armor, J. N.; Scheidegger, H.; Taube, H. *J. Am. Chem. Soc.* **1968,** *90,* 5928.

(14) (a) Cheney, R. P.; Armor, J. N. *Inorg. Chem.* **1977,** *16,* 3338. (b) Pell, S. D.; Armor, J. N. *J. Am. Chem. Soc.* **1975,** *97,* 5012.

124° IrNO angle and a formally Ir(III) oxidation state.[12] Although many linear NO^+ complexes of Ru(II) are known,[8] including the simple $[(NH_3)_5RuNO]^{3+}$ complex,[13] few ruthenium complexes of NO^- have been reported. The Ru(II) "dinitrosyl" $[RuCl(PPh_3)_2(NO)_2]^+$ complex has both bent NO^- and linear NO^+ ligands under fluxional interchange.[15,16] The remaining bent NO^- complexes of the 1980s were all strong-field Co(III) and second- or third-row organometallic species with singlet NO^- ligands.[20,21] Only recently have EXAFS studies of $[Fe(edta)NO]^{2-}$ [19] and EPR methods with related complexes[17,18] shown the existence of spin-polarized $Fe^{III}-(NO^-$ triplet) complexes, a category not recognized by MO treatments of the 1970s and 1980s. An interest in the reaction chemistry of NO^- toward metal centers has resurfaced with the biochemical observations that the NO/NO^- interconversion is catalyzed by superoxide dismutase[22] and that metmyoglobin is reduced by NO^- to the nitrosylated myoglobin, e.g. $[MbFe^{II}(NO^+)]$.[23]

Ruthenium nitrosyls are of current interest in medicine and in catalysis. $RuCl_3NO(H_2O)_2$ as a carrier of NO holds promise for the photodynamic therapy of solid tumors.[2] Ru^{III} polyamino polycarboxylate complexes are being used for the treatment of overproduction of NO during sepsis.[24] Fricker and co-workers have shown that $[Ru^{III}(edta)(H_2O)]^-$ scavenges NO rapidly ($k = 2 \times 10^7$ M^{-1} s^{-1}), forming $[Ru^{II}(edta)(NO^+)]^3$ and that salts of $[Ru^{III}(edta)Cl]^{2-}$ afford clinical protection of rats against lipopolysaccharide-induced septic shock.[1,3,24] Both Ru^{II} and Ru^{III} forms of $[Ru_2(ttha)(H_2O)_2]^{2-/0}$ ($ttha^{6-}$ = triethylenetetramine-hexaacetate) scavenge NO efficiently[4] for similar purposes. Meyer and co-workers have used $[Ru^{III}(edta)(H_2O)]^-$ to catalyze the electrochemical reduction of NO_2^- to NH_4^+, NH_2OH, and N_2O.[26] Coordinated HNO (protonated NO^-) was a proposed intermediate but was undetected in their study.[26]

Another area of interest with ruthenium nitrosyls is the nitrosyl−nitrite interconversion (eq 1). This reaction has been observed for ligand environments (L_n) as diverse as pentacyano,

$$L_nRu^{II}(NO^+) + 2OH \underset{}{\overset{K_{NO_2^-}}{\rightleftharpoons}} L_nRu^{II}(NO_2^-) + H_2O \quad (1)$$

polypyridyl, pentaammine, polyamino polycarboxylate, and violurate.[26−29] However, no unifying explanation concerning the value of $K_{NO_2^-}$ as a function of the ligand set has yet been provided. A recent attempt to rationalize the trend in $K_{NO_2^-}$ for the series *trans*-$[Ru^{II}(NH_3)_4L(NO)]^{3+}$ on the basis of σ-donation and π-acceptor power of L (L = L-histidine > imidazole > pyrazine > isonicotinamide > pyridine) showed an order favoring σ-donation over π-acceptor character but misplaced the position of pyrazine and pyridine by this explanation.[30]

In this paper, we present ^{15}N NMR, infrared, and electrochemical studies that allow us to detect and characterize distinct NO^+, NO, and NO^- complexes of $[Ru^{II}(hedta)]^-$. To our knowledge, this is a unique report wherein all three redox assignments of nitrosyl ligands with the entire NO^+, $NO^\bullet$, and NO^- series is known for a constant ligand−metal environment without changing the oxidation state of the metal for one or more of the three "NO" species. We have also been able to correlate ligand environment effects on the magnitude of $K_{NO_2^-}$ as long as the Ru(II) ammine series is excluded for reasons that are explained by H-bonding factors.

It is discussed herein that the type of coordinated NO^-, singlet or triplet, varies with the energy of NO π^* orbitals relative to the energy of d_{z^2} and $d_{x^2-y^2}$ metal orbitals in keeping with former MO treatments[20,32−35] and that singlet NO^- occurs when π-backbonding metal centers such as LS Ru^{II} are present, but not HS Fe^{II}. Thus, back-bonding stabilizes singlet NO^- as a ligand despite the previous conclusions that NO^- has little π-acceptor capability.[36−38] These studies extend the coordination chemistry of $[Ru^{II}(hedta)]^-$ that has recently shown several rarer bonding interactions with π-acceptor ligands including η^2-C≡N coordination to pyrimidines[39−41] and protonated pyrazines[42] and 1,4- or 1,3-metallotropic shifts with pyrazine[42a] and pyrimidine.[43]

Experimental Section

Reagents and Solutions. K[Ru(hedta)Cl] was prepared by a modification of our earlier reported procedure for Na[Ru(hedta)(H_2O)]·4H_2O by using KOH in place of NaOH upon workup.[44] Na_2[Ru_2(ttha)-

(15) Pierpont, C. G.; Eisenberg, R. *Inorg. Chem.* **1971**, *10*, 1088.

(16) Pierpont, C. G.; Van Derveer, D. G.; Durland, W.; Eisenberg, R. *J. Am. Chem. Soc.* **1970**, *92*, 4761.

(17) Bultitude, J.; Lackworthy, L. F.; Mason, J.; Povey, D. C.; Sandell, B. *Inorg. Chem.* **1984**, *23*, 3629.

(18) Bell, L. K.; Mason, J.; Mingos, D. M. P.; Tew, D. G. *Inorg. Chem.* **1983**, *22*, 2497.

(19) (a) Westre, T. E.; DiCicco, A.; Filipponi, A.; Natroni, C. R.; Hedman, B.; Solomon, E. I.; Hodgson, K. O. *J. Am. Chem. Soc.* **1994**, *116*, 6757. (b) Zhang, Y.; Pavlosky, M. A.; Brown, C. A.; Westre, T. E.; Hedman, B.; Hodgson, K. O.; Solomon, E. I. *J. Am. Chem. Soc.* **1992**, *114*, 9189.

(20) Shepherd, R. E.; Sweetland, M. A.; Junker, D. E. *J. Inorg. Biochem.* **1997**, *53*, 1.

(21) (a) Zang, Y.; Que, L. *Inorg. Chem.* **1995**, *34*, 1030. (b) Chiou, Y.-M.; Que, L. *Inorg. Chem.* **1995**, *34*, 3270.

(22) Murphy, M.; Sies, H. *Proc. Natl. Acad. Sci. U.S.A.* **1991**, *88*, 10860.

(23) Doyle, M. P.; Holkstra, J. W. *J. Inorg. Biochem.* **1981**, *14*, 351.

(24) (a) Fricker, S. P. *Platinum Met. Rev.* **1995**, *39*, 150. (b) Nathan, C. *FASEB J.* **1993**, *6*, 3051. (c) Moncada, S.; Palmer, R. M.; Higgs, E. A. *Pharmacol. Rev.* **1991**, *43*, 109. (d) Feldman, P. L.; Griffith, O. W.; Stuehr, D. J. Special Report: The Surprising Life of Nitric Oxide. *Chem. Eng. News* **1993**, *71* (Dec 20), 26−38. (e) Hibbs, J. B.; Taintor, R. R.; Vavrin, Z.; Rachlin, E. M. *Biochem Biophys. Res. Commun.* **1988**, *157*, 87. (f) Marletta, M.; Yoon, P. S.; Iyengar, R.; Leaf, C. D.; Wishnok, J. S. *Biochemistry* **1988**, *27*, 8706. (g) Stuehr, D. J.; Marletta. *Proc. Natl. Acad. Sci. U.S.A.* **1985**, *82*, 7738. (h) Crossin, K. L. *Trends. Biol. Sci.* **1991**, *16*, 81.

(25) (a) Farrell, N. P. In *Platinum and Other Metal Compounds in Cancer Chemotherapy*; Howell, S. B., Ed.; Plenum: New York, 1991; pp 81−91. (b) Farrell, N. P.; Qu, Y.; Van Houghton, B. *Biochemistry* **1990**, *29*, 9522. (c) Roberts, T. D.; Van Houghton, B.; Qu, Y.; Farrell, N. P. *Nucleic Acids Res.* **1989**, *17*, 9719. (d) Qu, Y.; Farrell, N. P. *Inorg. Chem.* **1995**, *34*, 3573. (e) Farrell, N. P.; Qu, Y.; Hacker, M. P. *J. Med. Chem.* **1990**, *33*, 2179.

(26) Rhodes, M. R.; Barley, M. H.; Meyer, T. J. *Inorg. Chem.* **1991**, *30*, 629.

(27) (a) Baraldo, L. M.; Bessega, M. S.; Rigotti, G. E.; Olabe, J. A. *Inorg. Chem.* **1994**, *33*, 5890. (b) Olabe, J. A.; Gentil, L. A.; Rigotti, G.; Navaza, A. *Inorg. Chem.* **1984**, *23*, 4297. (c) Chevalier, A. A.; Gentile, L. A.; Olabe, J. A. *J. Chem. Soc., Dalton Trans.* **1991**, 1959.

(28) (a) Godwin, J. B.; Meyer, T. J. *Inorg. Chem.* **1971**, *10*, 2150. (b) Pipes, D. W.; Meyer, T. J. *Inorg. Chem.* **1984**, *23*, 2466. (c) Leising, R. A.; Kubow, S. A.; Szczepura, L. F.; Takeuchi, K. J. *Inorg. Chim. Acta* **1996**, *245*, 167.

(29) Sueur, S.; Bremard, C.; Nowogrocki, G. *J. Inorg. Nucl. Chem.* **1976**, *38*, 2037.

(30) Gomes, M. G.; Davanso, C. U.; Silva. S. C.; Lopes, L. G. F.; Santos, P. S.; Franco, D. W. *J. Chem. Soc., Dalton Trans.* **1998**, 601.

(31) Curtis, J. C.; Sullivan, B. P.; Meyer, T. J. *Inorg. Chem.* **1983**, *22*, 224.

(32) Hoffmann, R. M.; Chen, M. M. L.; Elian, M.; Rossi, A. R.; Mingos, D. M. P. *Inorg. Chem.* **1974**, *13*, 2666.

(33) (a) Mingos, D. M. P.; Ibers, J. A. *Inorg. Chem.* **1971**, *10*, 1479. (b) Mingos, D. M. P. *Nature (London)* **1971**, *229*, 193.

(34) Mingos, D. M. P.; Robinson, W. T.; Ibers, J. A. *Inorg. Chem.* **1971**, *10*, 1043.

(35) (a) Haller, K. J.; Johnson, P. C.; Feltham, R. D.; Enemark, J. A. *Inorg. Chim. Acta* **1979**, *33*, 119. (b) Enemark, J. H.; Feltham, R. D.; Huie, B. T.; Johnson, P. L.; Swedo, K. B. *J. Am. Chem. Soc.* **1977**, *99*, 3285. (c) Hodges, K. D.; Wollman, R. G.; Kessel, S. L.; Hendrickson, D. N.; Van Derveer, D. G.; Barefield, E. K. *J. Am. Chem. Soc.* **1979**, *101*, 906. (d) Eisenberg, R. E.; Meyer, C. D. *Acc. Chem. Res.* **1975**, *8*, 26.

(36) Collman, J. P.; Fornham, P.; Dolcetti, G. *J. Am. Chem. Soc.* **1971**, *93*, 1788.

(37) Pierpont, C. G.; Eisenberg, R. *Inorg. Chem.* **1972**, *11*, 1088.

(38) Swinehart, J. H. *Coord. Chem. Rev.* **1967**, *2*, 713.

(39) Chen, Y.; Lin. F.-T.; Shepherd, R. E. *Inorg. Chem.* **1997**, *36*, 818.

(H$_2$O)$_2$] was available from prior studies.[5,45–47] Na^{15}NO$_2$ was obtained from Cambridge Isotope Laboratories with 98% enrichment in ^{15}N. NO gas was obtained in cylinders from Liquid Carbonic or Matheson/ Praxair. NO gas was passed through a solution of saturated Ca(OH)$_2$ or concentrated NaOH via needle dispersal below the solution surface to remove traces of NO$_2$. The entire line was prepurged with Ar or N$_2$ (Valley Welding Supply). The NO gas was bubbled through water after the hydroxide rinse to remove any Ca(OH)$_2$ or NaOH carryover in the gas stream.[4,20] Timed dispersal of NO through appropriate Ru^{II} samples was made either within Ar-purged, septum-sealed 10.0 mL round-bottom flasks or within the electrochemical cell compartment to prepare NO• complexes. Syringe methods and transfers of [Ru^{II}(hedta)L] samples to NMR tubes under Ar have been described previously.[39–43] Weighed amounts of Na^{15}NO$_2$ were sealed in 10.0 mL round-bottom flasks together with a rice-sized stirring bar. Reduced solutions, each prepared in D$_2$O and containing 1 equiv of [Ru^{II}(hedta)(D$_2$O)]$^-$, were syringed into the Na^{15}NO$_2$ container, the components were mixed magnetically, and the acidity was adjusted to a desired pD level using DCl or NaOH to generate the desired ^{15}NO$^+$ or ^{15}NO$_2$$^-$ complex for ^{15}N NMR study. In one series of experiments, the ^{15}NO$_2$$^-$:Ru^{II} ratio was varied from 0.81:1.0 to 3.0:1.0 to examine the samples for bis-substituted species. In later experiments, precisely measured 1.00:1.00 samples at a pD value starting at 3.0 were examined by ^{15}N NMR methods and recycled over Zn/Hg to promote reduction to coordinated ^{15}NO$^-$. The samples were then retransferred for NMR analysis in order to follow the growth of the [Ru^{II}(hedta)(^{15}NO$^-$)]$^{2-}$ complex from the original [Ru^{II}(hedta)(^{15}NO$^+$)] complex. A K$_2$[Ru^{II}(hedta)(NO$^-$)]·xH$_2$O sample for infrared study was prepared by Ar evaporation of a solution of K$_2$[Ru^{II}(hedta)(NO$^-$)] prepared as above and centrifuged to remove Zn(OH)$_2$ at pD ≅ 7.0. Samples of [Ru^{II}(hedta)(NO$^+$)]·xH$_2$O and Na[Ru(hedta)(NO$^+$)(NO$_2$$^-$)] as ^{15}N-labeled salts were obtained for infrared study by inducing precipitation of the desired complex by injecting Ar-purged absolute ethanol into the 1:1 or 1:2 sample under conditions matching those of the ^{15}N NMR experiments which detected these species in solution. K[Ru^{II}(hedta)(NO$^•$)]·xH$_2$O was brought out of solution using Ar-purged acetone to induce precipitation after NO was passed for 2.0 min through a K[Ru^{II}(hedta)(H$_2$O)] sample. Electrochemical studies showed this is sufficient time for complete NO complexation. The solids were ground with KBr to prepare pellets pressed at 9.0 tons. Samples were generally prepared to contain 2.50 × 10^{-2}–5.6 × 10^{-2} M [Ru^{II}(hedta)L] complex for ^{1}H NMR and 5.50 × 10^{-2} M for ^{13}C NMR and ^{15}N NMR. Samples from NMR tubes were transferred to 0.10 M NaCl, and the solutions were purged with N$_2$ or Ar, for electrochemical study at a 1:10 dilution relative to the NMR concentration. Alternately, samples solely for electrochemical studies were generated over Zn/Hg in 0.10 M NaCl Ar-purged electrolyte at ca. 2.50 × 10^{-3} M and transferred directly to the electrochemical cell and treated as described under Results and Discussion.

Instrumentation. ^{1}H NMR and ^{13}C NMR spectra were obtained on a Bruker AC300 spectrometer using standard procedures. The chemical shifts were calibrated against DSS (0.00 ppm) or HOD (4.80 ppm) for ^{1}H NMR and external dioxane (69.1 ppm) for ^{13}C NMR. ^{15}N NMR spectra were obtained on LD40 and Bruker AC300 spectrometers operating at 50.7 MHz. Calibration was made using ^{15}N-labeled formamide as the reference. A time delay of 120 s was used in the ^{15}N
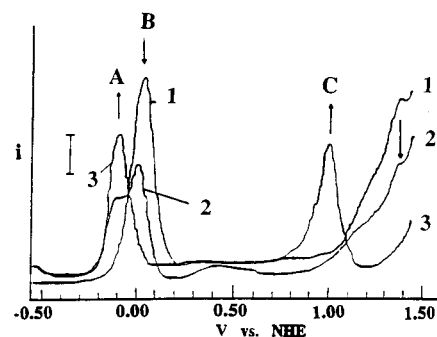
Figure 1. Electrochemical detection of NO coordination on [Ru^{II}-(hedta)(H$_2$O)]$^-$. Conditions for the differential pulse voltammograms: [Ru^{II} complex] = 2.61 × 10^{-3} M; T = 22 °C; μ = 0.10 (NaCl); time of 0 for the aqua complex; NO bubbling times of 40 and 95 s. Current marker = 20 μA. Times: (1) 0 s; (2) 40 s; (3) 95 s. Arrows: (A) −0.10 V; (B) +0.05 V; (C) +0.98 V.

data collection. Infrared spectra were recorded on a Perkin-Elmer IR32 instrument with an IR/30S peak pick subroutine. Spectra were compared to previously obtained spectra of Na[Ru(hedta)(H$_2$O)]·4H$_2$O and related complexes in order to assign carboxylate stretches and vibrations attributable to the [Ru^{II}(hedta)(H$_2$O)]$^-$ chromophore[46–48] that are background vibrations to those of coordinated NO$^+$, NO$^•$, NO$_2$$^-$, and NO$^-$. Electrochemical measurements were performed using an IBM 225 electrochemical analyzer with the standard three-electrode arrangement. A glassy-carbon electrode was the working electrode with a platinum wire auxiliary and an SCE reference electrode. Reported $E_{1/2}$ values are corrected to the NHE scale. Cyclic voltammograms were recorded at 50 mV s^{-1} sweep; differential pulse voltammograms were recorded at 40 mVs^{-1} using a 50 mV stepping voltage. Calibration techniques using the Ru$^{II/III}$ wave of [Ru(bpy)$_3$](ClO$_4$)$_3$ at 1.33 V and that of [Ru(hedta)(H$_2$O)]$^-$ at 0.05 V[49] were those described previously.[50]

Results and Discussion

The NO Complex of [Ru^{II}(hedta)]$^-$. When NO is admitted to a solution of 2.61 × 10^{-3} M [Ru^{II}(hedta)(H$_2$O)]$^-$ under Ar, a series of changes occurs in the differential pulse voltammograms (Figure 1). Initially waves are detected at +0.05 and ca. +1.39 V for the known Ru$^{II/III}$ and Ru$^{III/IV}$ waves of [Ru-(hedta)(H$_2$O)]$^-$.[46,49] But as NO replaces H$_2$O in the complex, these waves steadily decrease and new waves at $E_{1/2}$ values of −0.10 and +0.98 V vs NHE appear as shown by the voltammograms at 40 and 95 s of NO exposure. Data at other times of 10, 20, 65, and 125 s of NO bubbling produce intermediate and final spectra but are not shown for visualization clarity. At the final pH of 7.4, monitored by a mini-pH probe mounted into the electrochemical cell, these waves represent the Ru^{II}-(NO$^•$)/Ru^{II}(NO$^+$) couple at −0.10 V and the more complicated 2Ru^{II}(NO$_2$$^-$)/Ru^{III}(NO$^+$) + Ru^{III}(NO$_3$$^-$) wave at 0.98 V as described in previous reports for the {[Ru^{II}(NO)]$_2$(ttha)}$^{2-}$ system[4] and by Meyer and co-workers[51] and Nagao et al.[52] for ruthenium polypyridyl nitrosyl/nitrite complexes. The [Ru^{II}-(hedta)(NO$^•$)]$^-$ complex has the identical $E_{1/2}$ value reported for the structurally similar protonated edta^{4-} complex [Ru^{II}-

(40) (a) Zhang, S.; Holl, L. A.; Shepherd, R. E. *Inorg. Chem.* **1990**, *29*, 1012. (b) Shepherd, R. E.; Zhang, S.; Lin, F.-T.; Kortes, R. A. *Inorg. Chem.* **1992**, *31*, 1457.
(41) (a) Shepherd, R. E.; Chen, Y.; Zhang, S.; Kortes, R. A. In *Electron Transfer Reactions*; Isied, S., Ed.; Advances in Chemistry Series 253; American Chemical Society: Washington, DC, 1997; pp 367–398. (b) Shepherd, R. E.; Zhang, S. *Transition Met. Chem.* **1994**, *19*, 146.
(42) (a) Chen, Y.; Shepherd, R. E. *Inorg. Chem.* **1998**, *37*, 1249. (b) Chen, Y.; Shepherd, R. E. *Inorg. Chim. Acta* **1998**, *268*, 279.
(43) Chen, Y.; Lin, F.-T.; Shepherd, R. E. *Inorg. Chim. Acta* **1998**, *268*, 287.
(44) Zhang, S.; Shepherd, R. E. *Inorg. Chem.* **1988**, *27*, 4712.
(45) Zhang, S.; Shepherd, R. E. *Inorg. Chem.* **1994**, *33*, 5262.
(46) Zhang, S.; Shepherd, R. E. *Transition Met. Chem.* **1992**, *17*, 97.
(47) Chen, Y.; Zhang, S.; Shepherd, R. E. *Transition Met. Chem.* **1997**, *22*, 338.

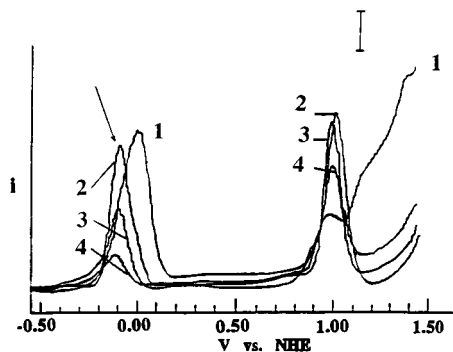(48) Zhang, S.; Shepherd, R. E. *Transition Met. Chem.* **1992**, *17*, 199.
(49) (a) Elliott, M. G.; Zhang, S.; Shepherd, R. E. *Inorg. Chem.* **1989**, *28*, 3036. (b) Zhang, S.; Holl, L. A.; Shepherd, R. E. *Transition Met. Chem.* **1992**, *17*, 390.
(50) Shepherd, R. E.; Zhang, S.; Dowd, P.; Choi, G.; Wilk, B.; Choi, S.-C. *Inorg. Chim. Acta* **1990**, *174*, 249.
(51) (a) Keene, F. R.; Salmon, D. J.; Walsh; Abruna, H. D.; Meyer, T. J. *Inorg. Chem.* **1980**, *19*, 1896. (b) Murphy, W. R.; Takeuchi, K. J.; Meyer, T. J. *J. Am. Chem. Soc.* **1982**, *104*, 5817.
(52) (a) Nagao, H.; Mukaida, M.; Shimuzu, K.; Howell, F. S.; Kakihara. *Inorg. Chem.* **1986**, *25*, 4312. (b) Ooyama, D.; Nagao, N.; Nagao, H.; Miura, Y.; Hasegawa, A.; Ando, K.-I.; Mukaido, M.; Tanaka, K. *Inorg. Chem.* **1995**, *34*, 6024.
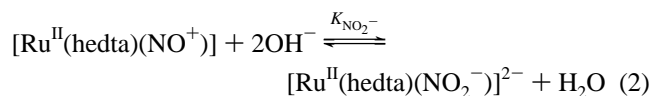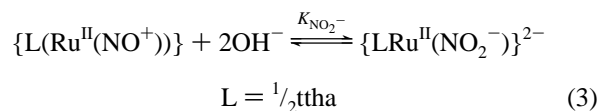
Figure 2. Electrochemical detection of the NO^+/NO_2^- equilibrium and its pH dependence for $[Ru^{II}(hedta)(NO^+)]$. Differential pulse voltammograms were recorded under the same conditions as those for Figure 1 at pH = 6.0 (1) for $[Ru^{II}(hedta)(H_2O)]^-$ and at pH = 2.90 (2), 7.40 (3), and 9.90 (4) for the NO complex prepared by admission of NO for 180 s followed by brief Ar purging to remove excess NO and pH adjustment. Current marker = 20 μA; arrow denotes the $[Ru(hedta)-(NO)]^-/[Ru(hedta)(NO^+)]$ wave.

$(Hedta)(NO\cdot)]^{2-}.^{26}$ The exposed nitrosyl of $[Ru^{II}(hedta)(NO\cdot)]^-$ is more readily oxidized than when the $Ru^{II}(NO)$ chromophore is imbedded inside a polytungstate; $E_{1/2}$ is shifted to 0.05 V for the same wave for $[SiW_{11}O_{39}Ru^{II}(NO\cdot)]^{6-}.^{53}$

It was observed that the amplitude of the −0.10 V wave present in the $[Ru^{II}(hedta)(NO\cdot)]^-/[Ru^{II}(hedta)(NO^+)]$ oxidation varied with pH as shown in Figure 2. However, the complex wave of the further oxidation near 1.0 V is not sensitive to pH except by dilution caused by addition of purged NaOH or HCl to shift the pH to various desired values. The explanation for the amplitude change at −0.10 V is given by the competitive equilibrium forming the nitro complex from a portion of the $[Ru^{II}(hedta)(NO^+)]$ species within the monolayer of the glassy-carbon electrode sensor as given in eq 2. As the equilibrium

$$[Ru^{II}(hedta)(NO^+)] + 2OH^- \xrightleftharpoons{K_{NO_2^-}}$$
$$[Ru^{II}(hedta)(NO_2^-)]^{2-} + H_2O \quad (2)$$

shifts toward the nitro complex, the electroactive $[Ru^{II}(hedta)-(NO^+)]$ species available for redox equilibrium with $[Ru^{II}-(hedta)(NO\cdot)]$ is decreased. Therefore, at higher pH, the amplitude for the −0.10 V wave is suppressed, compared to the amplitude of the wave for the total redox-active forms at 0.98 V where both $[Ru^{II}(hedta)(NO^+)]$ and $[Ru^{II}(hedta)(NO_2^-)]^{2-}$ are oxidized to $[Ru^{III}(hedta)(NO^+)]$ and $[Ru^{III}(hedta)(ONO_2^-)]^-$. From the −0.10 V wave amplitude at pH = 2.90, representing total Ru^{II} present at $[Ru^{II}(hedta)(NO^+)]$, and wave heights as a function of pH representing the various amounts of $[Ru^{II}(hedta)-(NO^+)]$ and, by difference, the amount of $[Ru^{II}(hedta)(NO_2^-)]^{2-}$ at equilibrium, the value of $K_{NO_2^-}$ was calculated to be 1.44×10^{13} M^{-2} for equilibrium 2. A related set of experiments were performed using a two-independent-site model for the similar equilibrium of $\{[Ru^{II}(NO^+)]_2(ttha)\}$ converting to its nitro complex (eq 3). From the pH-dependent amplitudes of the −0.06

$$\{L(Ru^{II}(NO^+))\} + 2OH^- \xrightleftharpoons{K_{NO_2^-}} \{LRu^{II}(NO_2^-)\}^{2-}$$
$$L = {}^1/_2 ttha \quad (3)$$

V wave of this complex, representing the analogous $Ru^{II}(NO\cdot)/Ru^{II}(NO^+)$ electrochemical change,[5] the value of 4.53×10^{12}

Table 1. $K_{NO_2^-}$ Formation Constants and Related ν_{NO} Data

	K	NO str, cm^{-1}	ref
$[Os(CN)_5NO]^{2-}$	42	1897	27a
$[Ru(CN)_5NO]^{2-}$	4.4×10^6	1926	27b,c
$[RuCl(bpy)_2NO]^{2+}$	1.6×10^9	1927	28a
$[Os(terpy)(bpy)NO]^{3+}$	7.0×10^7	1904	28b
$[Ru_2(ttha)(NO)_2]$	4.5×10^{12}		this work
$[Ru(hedta)(NO)]$	1.44×10^{13}	1846	this work
$[Ru(terpy)(bpy)NO]^{3+}$	2.1×10^{23}	1952	28b
$[Fe(CN)_5NO]^{2-}$	1.5×10^6	1945	73, 74
free NO^+		2377	7
free NO		1876	7, 60
free NO^-		1470	7
$[Fe(edta)(NO)]^{2-}$		1776	19b

M^{-2} for equilibrium 3 was obtained. An estimate of $K_{NO_2^-}$ for the $[Ru^{II}(edta)(NO^+)]/[Ru^{II}(edta)(NO_2^-)]$ equilibrium of 1.0×10^9 M^{-2} can be obtained from Meyer's data.[26] Values of $K_{NO_2^-}$ obtained from literature sources and this present work are given in Table 1 along with the infrared stretch (ν_{NO}) of the nitrosyl form of these complexes.
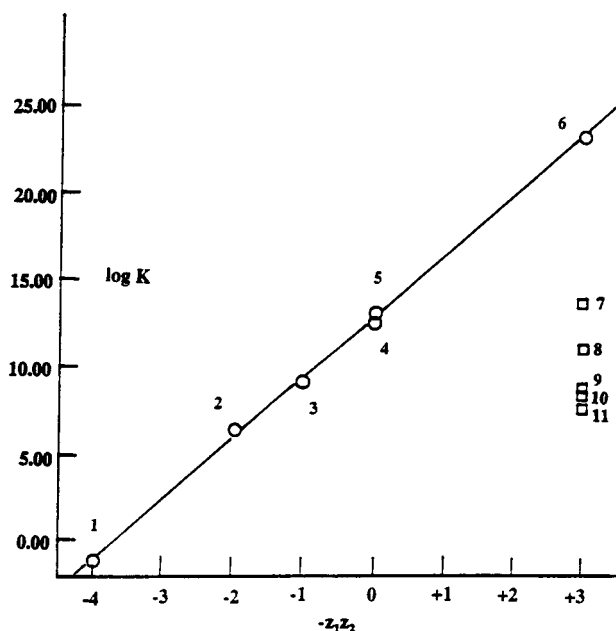
As anticipated from equilibrium 3, it was shown that the high-pH form of the complex could be obtained by the addition of NO_2^- to $[Ru^{II}(hedta)(H_2O)]^-$ or $[Ru^{II}_2(ttha)(H_2O)_2]^{2-}$ as shown in Figure SF-1 of the Supporting Information. The low-amplitude wave at ca. −0.10 V matches the amplitude and response throughout the voltage scan of those for the "high-pH" form (pH = 9.90) when $[Ru^{II}(hedta)(NO^+)]$ is produced at the glassy carbon surface via NO addition to $[Ru^{II}-(hedta)(H_2O)]^-$ and its subsequent electrochemical oxidation. A minor wave at −0.37 V is observed, which from later evidence is ascribed to the $[Ru^{II}(hedta)(NO^-)]^{2-}/[Ru^{II}(hedta)-(NO\cdot)]^-$ couple. When $NaNO_3$ is added to a solution of $[Ru^{II}(hedta)(H_2O)]^-$, no change in the waves of the aqua complex, and hence no coordination of NO_3^-, occurs with the Ru^{II} form of the complex.

A Unified Explanation for Trends in $K_{NO_2^-}$. The values of $\log(K_{NO_2^-})$ for various $Ru^{II}(NO^+)$ complexes of Table 1 exhibit a linear relationship as a function of minus the charge product for the nitrosyl complex and OH^- ($-z_1z_2$) as shown in Figure 3. The linearity is strictly obeyed from $-z_1z_2$ of −4 for the violurate complex[29] to +3 for the $[Ru(terpy)(bpy)NO]^{3+}$ complex[28] and tracks through the charge product of 0 and $\log(K_{NO_2^-})$ values for the $[Ru^{II}(hedta)(NO^+)]$ and $\{[Ru^{II}(NO^+)_2-(ttha)\}$ complexes determined herein. An explanation for this behavior is that $K_{NO_2^-}$ is a composite constant of $K = K_{OH^-}K_T$. K_{OH^-} represents the equilibrium constant for an electrostatically controlled OH^- addition equilibrium, followed by a proton-transfer step for the second OH^- of the equilibrium. Due to the observed linearity of Figure 3, it follows that K_T is virtually constant for all $LRu(HONO)$ complexes.

$$[LRu^{II}(NO^+)]^n + OH^- \xrightleftharpoons{K_{OH^-}} [LRu^{II}(NO(OH))]^{n-1} \quad (4a)$$

$$[LRu^{II}(NO(OH))]^{n-1} + OH^- \xrightleftharpoons{K_T} [LRu^{II}(NO_2^-)]^{n-2} + H_2O \quad (4b)$$

The observed dependence with $\log(K_{NO_2^-})$ linear in $-z_1z_2$ will be obeyed when K_{OH^-} follows the electrostatic ion-pairing constant function[54]

(53) Filipek, K. *Inorg. Chim. Acta* **1995**, *231*, 237.

(54) (a) Wilkins, R. G. *The Study of Kinetics and Mechanism of Reactions of Transition Metal Complexes*; Allyn and Bacon: Boston, MA, 1974; pp 182−183. (b) Beck, M. T. *Coord. Chem. Rev.* **1968**, *3*, 91.

Figure 3. Correlation of the NO$^+$/NO$_2^-$ equilibrium constant of Ru^{II}L complexes with the charge product $-z_1z_2$ for hydroxide attack. (Literature values for log($K_{NO_2^-}$) were obtained as in Table 1.) Complexes: (1) [Ru(violurate)$_2$Cl(NO)]$^{4-}$; (2) [Ru(CN)$_5$NO]$^{2-}$; (3) [Ru(edta)(NO)]$^-$; (4) {[Ru(NO)]$_2$(ttha)}; (5) [Ru(hedta)(NO)]; (6) [Ru(terpy)(bpy)(NO)]$^{3+}$; (7–11) [Ru(NH$_3$)$_4$L(NO)]$^{3+}$, with L = (7) histidine, (8) imidazole, (9) pyrazine, (10) pyridine, and (11) isonicotinamide.

$$K_{OH^-} = \left(\frac{4\pi Na^3}{3000}\right)\exp\left[-\frac{(z_1z_2e^2/aD) - z_1z_2e^2\kappa/D(1+\kappa a)}{kT}\right] \tag{5}$$

To a first approximation, the slope of such lines equals $e^2/aDkT$ [54,55] where a is the "distance of closest approach" between the charge centers. From the slope of 3.44 in Figure 3, the bulk dielectric constant of 78, $e = 4.803 \times 10^{-10}$ esu, and 298.16 K, we calculate $a = 2.09$ Å, comparable in magnitude to 4.3 Å for the ion-pairing distance of Co-(NH$_3$)$_6^{3+}$,Cl$^-$.[55] The calculated a value is perhaps fortuitously close to the typical Ru^{II}–N bond distance, recognizing that the site of OH$^-$ addition is the coordinated N of the NO$^+$ unit. The accuracy of such an ion-pairing model is likely to be solvation-sensitive for the approaching ions. It may be proper to limit the conclusion in this case to the idea that OH$^-$ must be very close to the Ru^{II}(NO$^+$) reaction center rather than an exact distance.

The estimate of 2.09 Å for a permits calculation of $K_{OH^-} \cong 2.30 \times 10^{-2}$ and hence $K_T = 6.26 \times 10^{14}$, from which an estimate of K_a for HONO coordinated to [Ru^{II}(hedta)]$^-$ of 6.26 can be made. Thus, the pK_a of the N-coordinated nitrous acid is -0.80. Since the pK_a of free HNO$_2$ is 3.15,[56] the coordination of Ru^{II} in the [Ru^{II}(hedta)(NO(OH))]$^-$ complex enhances the HONO acidity by 3.85 log units. This is in reasonable agreement with the electrostatic influence of M^{2+} centers on the acidification of coordinated small HX units such as H$_2$O wherein the hydroxy MOH$^+$ species often begins to form near pH $\cong$ 10 (e.g., pK_a values are for Fe(H$_2$O)$_6^{2+}$ 9.5, Zn(H$_2$O)$_6^{2+}$ 9.0, Cd-(H$_2$O)$_6^{2+}$ 10.0, and Cu(H$_2$O)$_6^{2+}$ 8.0, compared to 15.7 for
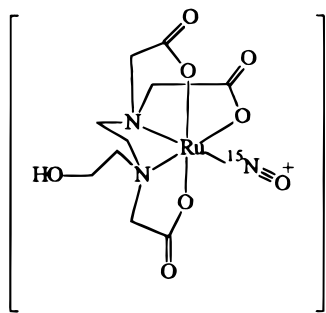
(55) (a) Basolo, F.; Pearson, R. G. *Mechanisms of Inorganic Reactions*; Wiley: New York, 1967; p 36. (b) Caton, J. A.; Prue, J. E. *J. Chem. Soc.* **1956**, *671*.
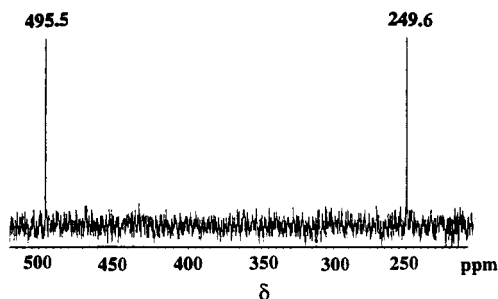(56) Harris, D. C. *Quantitative Chemical Analysis*, 2nd ed.; Freeman: New York, 1987; p 735.

H$_2$O).[55,56] Since the anionic hedta^{3-} ligand somewhat compensates the Ru^{II} center, its influence on acidification of small molecules such as H$_2$O or HONO will be slightly less. Thus the decrease of 3.85 log units in the pK_a of HNO$_2$ vs [Ru^{II}(hedta)(HNO$_2$)]$^-$ is properly less than 5.7 units for H$_2$O within Cd(H$_2$O)$_6^{2+}$, a central ion of virtually the same size as Ru^{II}.

Examination of the NO frequencies of the NO$^+$ complexes of Table 1 reveals that [Ru^{II}(hedta)(NO$^+$)] with $\nu_{NO} = 1846$ cm^{-1} has a lower frequency than [Ru(CN)$_5$NO]$^{2-}$ (1926 cm^{-1}) and the polypyridyl type of Ru^{II}(NO$^+$) complexes (1927–1952 cm^{-1}). In fact, the NO frequency of the [Ru^{II}(hedta)(NO$^+$)] complex is lower than that of free NO· (1876 cm^{-1}) but above 1776 cm^{-1}, that of the Fe^{III}–triplet NO$^-$ complex of [Fe-(edta)NO]$^{2-}$.[19b] One can infer that [Ru^{II}(hedta)(NO$^+$)] has substantial resonance components of Ru^{IV}(NO$^-$) and Ru^{III}-(NO·) from among the following contributors, which lowers ν_{NO} significantly:

$$[(hedta)Ru^{II}(NO^+)] \leftrightarrow [(hedta)Ru^{III}(NO\cdot)] \leftrightarrow$$
$$[(hedta)Ru^{IV}(NO^-)]$$

By contrast, the polypyridyl ruthenium nitrosyls have larger contributions from the analogous LRu^{II}(NO$^+$) resonance forms.

It can be seen from the data in Table 1 that the Os^{II} analogues exhibit smaller $K_{NO_2^-}$ values than their Ru^{II} counterparts. Assuming a similar linear response to $-z_1z_2$ for log($K_{NO_2^-}$), one obtains a slope of 1.23 for Os^{II} as a series (not shown in Figure 3) compared to 3.44 for Ru^{II}. This implies an a value of 5.85 Å and K_{OH^-} of 0.84 for a theoretical [Os^{II}(hedta)(NO$^+$)] complex for which a graphical value of $K_{NO_2^-} = 1.0 \times 10^4$ was obtained. This predicts that the pK_a of [Os^{II}(hedta)(NO(OH))]$^-$ would be 9.92 and hence the stable form at neutral pH, whereas the pK_a of [Os(terpy)(bpy)(NO(OH))]$^{2+}$ would be 6.08. In concert with this view, the experimental evaluation of the [Os(terpy)(bpy)-(NO$^+$)]$^{3+}$/[Os^{II}(terpy)(bpy)(NO$_2^-$)]$^+$ equilibrium was determined from pH 7.4 to 11.00,[28b] outside the range of significant interference by a competitive [Os^{II}(terpy)(bpy)(NO(OH))]$^{2+}$ formation. The larger calculated a value for the Os^{II} series compared to Ru^{II} suggests the OH$^-$ entering group sees an LOs^{II}-(NO$^+$) species with less NO$^+$ character and hence resides in a precursor ion pair at a longer distance than that for LRu^{II}(NO$^+$). The concept of less positive charge on the NO$^+$ of the Os^{II} series is in agreement with spectroscopic evidence. From the infrared data, one can infer that greater contributions of the Os^{III}(NO·) and Os^{IV}(NO$^-$) resonance forms occur, equivalent to greater back-bonding from the Os center, than for the Ru^{II} counterparts. This conclusion was previously mentioned by Pipes and Meyer on the bases of electrochemical, spectral, and reactivity differences in comparison with Ru^{II} nitrosyl/Ru^{II} nitrite equilibria.[28b]

When the values of $K_{NO_2^-}$ for the tetraammine series of Franco and co-workers[30] are added to the plot of Figure 3, all of the data points for the [LRu^{II}(NH$_3$)$_4$(NO$^+$)]$^{3+}$ species fall well below the linear data for other Ru^{II}(NO$^+$) complexes of the violurate, pentacyano, polyamino polycarboxylate, or polypyridyl series. If the [LRu^{II}(NH$_3$)$_4$(NO$^+$)]$^{3+}$ species were to form stronger H-bonds between ammonia ligands and the solvent cage than for the less positively charged [LRu^{II}(NH$_3$)$_4$(NO$_2^-$)]$^+$ product, a free energy barrier which favors the nitrosyl form, and hence smaller values of $K_{NO_2^-}$, will be established. The values of $K_{NO_2^-}$ for the tetraammine series are between 10 and 15 log units lower than those of the other 3+ cationic ruthenium nitrosyls. This corresponds to a change in solvation between 5.9 and 8.9 kcal/mol. Estimates based on the selective solvation of ruthenium-

(II/III) ammines vs ruthenium(II/III) polypyridyls[31] have shown that the barrier increases with the number of NH_3 ligands and that barriers as large as 32 kcal/mol are readily achieved.[31] Thus, the similar influence upon solvation of $[LRu(NH_3)_4(NO^+)]^{3+}$, a 3+ ion, changing to that of a 1+ cation as implied for $K_{NO_2^-}$ is well within a solvent barrier explanation as to why the tetraammine ruthenium nitrosyls depart from the behavior clearly established for more insulating ligands (CN^-, hedta, terpy, etc.).

NMR Studies of Coordinated NO Species with [Ru^{II}-(hedta)]$^-$. We turned to the ^{15}N NMR method to obtain a more straightforward estimate of the nature of the electron density at the coordinated NO ligand. Previous researchers have shown that when linear NO^+ is coordinated, $^{15}NO^+$-bound complexes resonate near 250 ppm (257 ppm for $[(NH_3)_5RuNO]^{3+}$ and 228 ppm for $[RuCl_5NO]^{2-}$), coordinated $^{15}NO_2^-$ resonates near 348 ppm, and coordinated $^{15}NO^-$ resonates between 600 and 700 ppm[17,18]—all referenced to [^{15}N]formamide.[58]

When labeled $Na^{15}NO_2$ is combined with $[Ru^{II}(hedta)-(D_2O)]$ in a ratio of 0.80 or 1.0 ($Na^{15}NO_2$:Ru^{II}) at pD ≤ 3.0, the ^{15}N NMR spectrum shown in Figure 4 is obtained. A single resonance appears at 249.6 ppm. Also shown is an external $Na^{15}NO_2$ reference at 495.5 ppm. The electrochemical data show that all of the $[Ru^{II}(hedta)(^{15}NO_2^-)]^{2-}$ complex will convert to $[Ru^{II}(hedta)(^{15}NO^+)]$ at pD ≤ 3.0. The ^{15}N NMR further confirms the initial presence of a single isomer as the coordinated $^{15}NO^+$ species having the 249.6 ppm resonance and no $^{15}NO_2^-$-coordinated species which would appear in the 350 ppm range. Separate 2-D NMR and HC-COLOC spectra clearly identify three coordinated carboxylate carbons (^{13}C NMR shifts at 187, 183, and 182 ppm), three AB ^1H NMR patterns for the coordinated glycinato arms with the glycinato arm cis to the NO^+ ligand as the most downfield. Therefore the structure is unambiguously cis-equatorial as shown here by the combination of ^{15}N, ^{13}C, and ^1H NMR techniques:
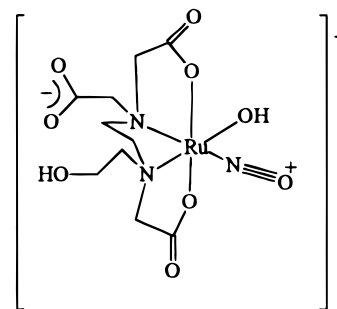

After 8 h in contact with Zn/Hg, with a pD rise to 6.0, the 249.6 ppm resonance decreases, forming three new species with resonances at 270.6, 255.3, and 253.8 ppm in the ratio 49:30:21 (Figure SF-2 in the Supporting Information). It is known from former studies[42] that strong π-acceptor ligands such as CO and NO^+ induce one stereochemical arrangement of the $[Ru^{II}(hedta)]^-$, the cis-equatorial isomer, which exhibits three coordinated carboxylates having ^{13}C NMR resonances near 188 ppm. The distribution of stereochemical isomers involving the $[Ru^{II}(hedta)L]^-$ complexes is shown in Figure SF-3 of the Supporting Information. Molecular mechanical interactions for L = H_2O establish the ratio of the three isomers to be 44:39:17 (cis-equatorial:trans-equatorial:cis-polar). Cis-equatorial is least strained and highly stabilized by strong π-acceptor ligands such

(57) Douglas, B. E.; McDaniel, D.; Alexander, J. *Concepts and Models of Inorganic Chemistry*, 3rd ed.; Wiley: New York, 1994; p 331.
(58) Typical shifts reported in refs 17 and 18, referenced to nitromethane, have been adjusted to the formamide reference of this report.

Figure 4. ^{15}N NMR spectrum of $[Ru^{II}(hedta)(H_2O)]^-$ and $Na^{15}NO_2$ mixed at 1.00:0.80 at pD < 3.0. The spectrum was obtained immediately after mixing; [complex] = 2.50×10^{-2} M; T = 25 °C. The mononitrosyl complex resonance at 249.6 ppm, and the external $^{15}NO_2^-$ marker is at 495.5 ppm.

as CO or NO^+. In these two cases, only three carboxylates are observed near 188 ppm and only seven carbons of the cis isomer appear between 25 and 70 ppm in the ^{13}C spectrum. Weaker π-acceptor ligands which are also stronger σ-donors than H_2O can stabilize the trans-equatorial and cis-equatorial isomers nearly the same. Hence, two isomers appear for weaker π-acceptors, including NO^- of this report. Weakly bonding, fluxionally coordinated ligands stabilize the cis-polar form as described elsewhere.[42] The formation of three different species from the initial one resonating at 249.6 ppm, all with resonances in the range demanded by coordinated $^{15}NO^+$, is explained by the labilization of each of the three cis carboxylate groups of the one cis-equatorial $[Ru^{II}(hedta)(^{15}NO^+)]$ complex. Displacement with coordination of H_2O or OH^- at the three different positions accounts for the slow loss of the 249.6 ppm resonance at the expense of the growing set of three (270.6, 255.5, and 253.8 ppm). Since the formation of these species can be reversed by acidification from pD 6.0 to pD 2.0, it is evident that the ligand which replaces the carboxylate donor is OH^-. One of the three isomers will be as shown; experience with other π-acceptor ligands suggests that this will be the species of 49% abundance with lesser dissociation occurring from the axial carboxylate positions:
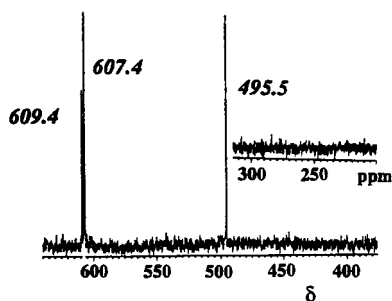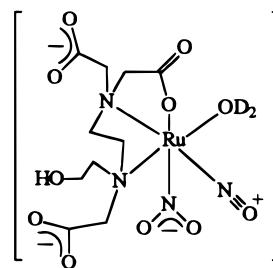

In the same 8 h period, a lesser amount of slowly growing species with resonances at 609.4 and 607.4 ppm was observed. The amount of the 609/607 pair was increased by the presence of excess $[Ru^{II}(hedta)(D_2O)]^-$ acting as a reducing agent. It was shown that excess Ru^{II} is not needed if the reducing agent is supplied by Zn/Hg instead.

Increasing the contact with Zn/Hg with periodic pD adjustment with DCl to maintain a freshly exposed Zn/Hg surface led to a complete conversion of the $[Ru^{II}(hedta)(^{15}NO^+)]$ complex to the species of the 609.4/607.4 resonance at 1:1 stoichiometry (Figure 5). The value of the ^{15}N chemical shift is correct for an $^{15}NO^-$ complex. Less strong π-acceptor ligands, but ones which are also good σ-donors, stabilize cis-equatorial

Figure 5. ^{15}NMR spectrum of [Ru^{II}(hedta)(NO$^-$)]$^{2-}$ at pD $\cong$ 7.0. [Complex] $= 2.50 \times 10^{-2}$ M; $T = 25$ °C; prepared at 1:1 with Na^{15}NO$_2$ over Zn/Hg (see text). The inset shows the blank region near 250 ppm for the absence of any NO$^+$ complex. The 609/107 ppm pair is for the isomers of the NO$^-$ complex; 495.5 ppm is the NO$_2^-$ reference marker.

and trans-equatorial forms of [Ru^{II}(hedta)X] complexes in approximately equal amounts which vary slightly with ligand X.[42,59] The ^{13}C spectrum of the ^{15}N sample that has been converted to [Ru^{II}(hedta)(^{15}NO$^-$)] is presented in Figure SF-4 of the Supporting Information. There are two sets of three carboxylate carbonyl carbon resonances at 184, 181, and 178 ppm and two sets of seven resonances for the other seven hedta^{3-}-based C centers occurring between 54.9 and 70.4 ppm. This establishes that all three carboxylates of [Ru^{II}(hedta)] are coordinated in $\geq$85% of the [Ru^{II}(hedta)(^{15}NO$^-$)] complexes which are cis-equatorial or trans-equatorial isomers. However, a minor (15%) species requiring one dissociated carboxylate arm appears with resonances near 175 ppm. Since the extent of labilization is only 15% compared to an equilibrium amount of 100% cis-labilization for ^{15}NO$^+$ and other strong π-acceptors such as η^2-bound pyrimidines promote the loss of one cis in-plane carboxylate,[39–41,43] from the small amount of cis-labilization by NO$^-$ it can be interpreted that NO$^-$ is a much poorer π-acceptor than NO$^+$—a clearly anticipated result. However, the sharp-line ^{15}N NMR spectrum of [Ru^{II}(hedta)(^{15}NO$^-$)] shows that the ^{15}NO$^-$ ligand is a singlet species. For the iron family, NO$^-$ is favored as a singlet only by back-donation. Without back-donation, electron repulsions force formation of the NO$^-$ triplet species which occurs upon coordination of NO to weak-field Fe^{II} complexes.[15,20,21] But when back-donation is possible, the d-orbital splitting favors singlet NO$^-$ or NO$^+$ depending upon the total electrons available in the {MNO}^{n} units and the energies of d$_{z^2}$ and d$_{x^2-y^2}$ orbitals relative to π* MO's of NO. Thus, although NO$^-$ must act as a much poorer π-acceptor than NO$^+$, the magnitude of the interaction is nonzero and sufficiently high to form the NO$^-$ singlet with Ru^{II}.
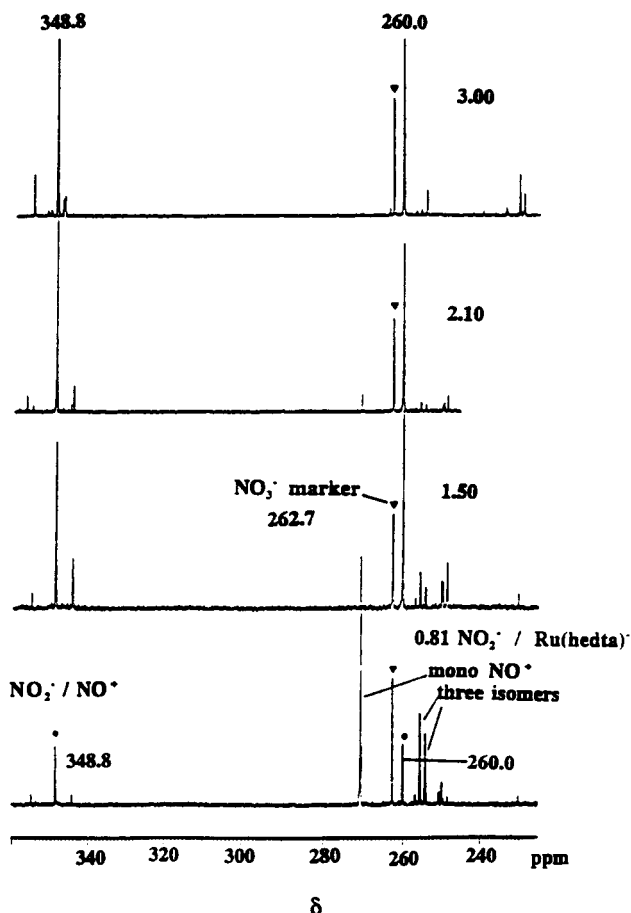
^{15}N NMR Spectrum of [Ru^{II}(hedta)(^{15}NO$^+$)(^{15}NO$_2^-$)]. Since the ^{15}NO$^+$ ligand labilizes cis-carboxylate donors, the possibility of adding an additional NO$^+$ or NO$_2^-$ ligand was studied using Na^{15}NO$_2$:[Ru^{II}(hedta)]$^-$ ratios of 0.81, 1.50, 2.10, and 3.00 as shown in Figure 6. In these studies, a contaminant of Na^{15}NO$_3$ was present. However, the "contaminant" served as a useful internal standard which resonates at 262.7 ppm (determined for authentic Na^{15}NO$_3$). The absence of coordination of ^{15}NO$_3^-$ to [Ru^{II}(hedta)]$^-$ confirms the electrochemical observations. The 262.7 ppm ^{15}NO$_3^-$ marker remained constant in all four ratios of Figure 6. Mixing of solid Na^{15}NO$_2$ into [Ru^{II}(hedta)(D$_2$O)]$^-$ within NMR tubes produced a local mixing effect that induces some "disubstituted nitrite" complexation even for the 0.81:1.00 sample. However, all observations

confirmed results described above. In the LRu^{II}(NO$^+$) region at 0.81:1.00, there evolved the three main resonances of the monosubstituted [Ru^{II}(hedta)(NO$^+$)] species having one displaced carboxylate donor. Additionally, a smaller amount of a species with two equally intense resonances at 348.8 and 260.0 ppm was present. The positions of these shifts of the minor species are indicative of a coordinated ^{15}NO$_2^-$ and a coordinated ^{15}NO$^+$ ligand, respectively. As the ratio of ^{15}NO$_2^-$:[Ru^{II}(hedta)]$^-$ was increased from 0.81:1.00 to 1.50:1.00 and 2.10:1.00, the resonances for the three monosubstituted [Ru(hedta)(^{15}NO$^+$)] species decreased to nearly zero while the pair of resonances for the disubstituted species grew to virtually 100% of the species present. At 3.00:1.00, no major amount of any additional species was noted. A sample of 2.00:1.00 Na^{15}NO$_2$:[Ru^{II}-(hedta)]$^-$, which was prepared by slow mixing of Na^{15}NO$_2$ dissolved in D$_2$O to lessen side reaction products, was examined by ^{13}C NMR. Three resonances were detected at 184, 175, and 173 ppm, indicating that two carboxylate arms are pendant and only one is coordinated in the [Ru^{II}(hedta)(^{15}NO$_2^-$)(^{15}NO$^+$)] complex. Given the ability of NO$^+$ to labilize the cis position, its original addition in-plane with the en backbone, and the requirement to have two pendant carboxylate groups, the structure shown here is predicted for this complex:

A 125 MHz/500 MHz CH-COLOC spectrum and a 2-D ^{1}H NMR spectrum confirmed that the coordinated carboxylate is a neighbor of a pendant carboxylate and that the second pendant carboxylate is a neighbor of the pendant alcohol functionality. This rules out other structural possibilities where both pendant carboxylates occur at the nitrogen trans to NO$^+$ or where the carboxylate donor coordinates to the nitrogen possessing the alcohol arm. We cannot rule out the possibility that the "axial" carboxylate and bound D$_2$O are not interchanged. However, all strong π-acceptors labilize the "in-plane" carboxylate, favoring the given structure.
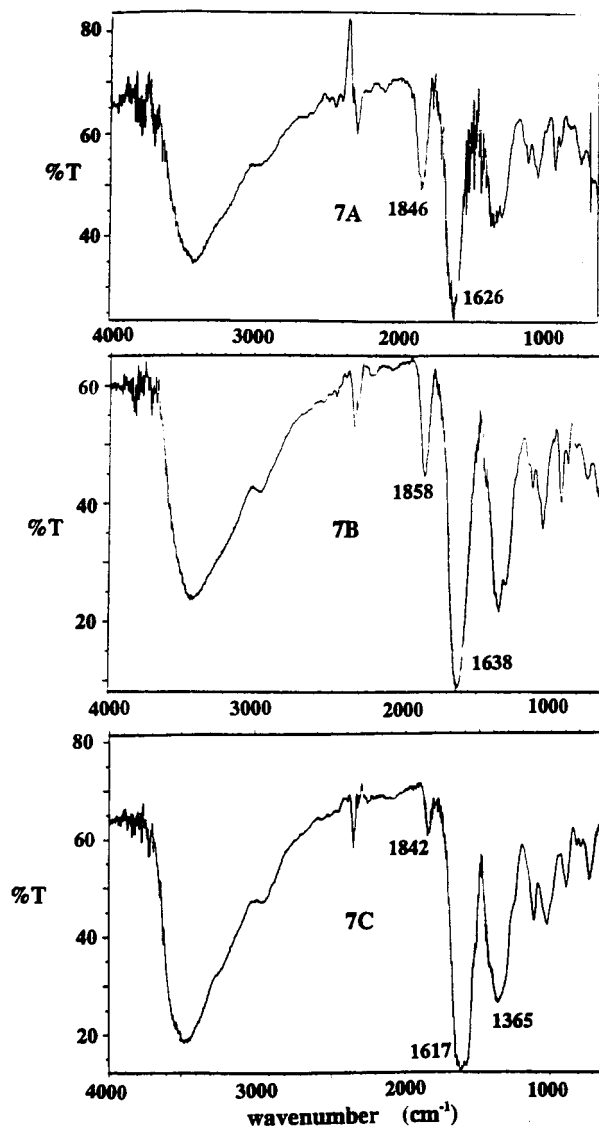
Infrared Spectra of Coordinated NO Species. Solid samples were prepared by forcing the highly soluble [Ru^{II}-(hedta)(NO)] species to precipitate upon changing the dielectric constant of the solvent water by adding ethanol or acetone. The solubility of these species was promoted by the pendant alcohol functionality and, in several cases, the presence of other pendant carboxylate groups in the desired Ru–NO species of interest. Na[Ru^{II}(hedta)(^{15}NO$^+$)(^{15}NO$_2^-$)]·xH$_2$O was obtained by this method. A slower evaporation method gave K$_2$[Ru^{II}(hedta)-(^{15}NO$^-$)]·xH$_2$O. The infrared spectra of these solids are shown in Figure SF-5 of the Supporting Information and in Figure 7C, respectively. For Na[Ru(hedta)(^{15}NO)(^{15}NO$_2$)], ν_{NO} of the ^{15}NO$^+$ ligand appears as an easily resolved band at 1827 cm^{-1}, a higher frequency than that of the coordinated carboxylates at 1632 cm^{-1}. The coordinated ^{15}NO$_2^-$ ligand is detected by two sharp stretches at 1370 and 1300 cm^{-1}. The parent Na[Ru^{II}(hedta)-(H$_2$O)] complex has four stretches in this region, but these are half the intensity of those when ^{15}NO$_2^-$ is coordinated. The assignments have been made following those of Mukaida and co-workers.[52b] The ν_{as}(NO$_2$) and ν_s(NO$_2$) stretches have been

(59) Shepherd, R. E.; Zhang, S. *Inorg. Chim. Acta* **1992**, *191*, 271.

Figure 6. Formation of $[Ru^{II}(hedta)(^{15}NO^+)(^{15}NO_2^-)]^-$ as detected by ^{15}N NMR. [Complex] = 2.50×10^{-2} M with Ru^{II}:$^{15}NO_2^-$ ratios of 0.81:1.00, 2.10:1.00, and 3.00:1.00; $T = 25$ °C.

Figure 7. Infrared spectra of $[Ru^{II}(hedta)X]^{n-}$ complexes as K^+ salts (X: NO^+, $n = 0$; $NO\cdot$, $n = 1$; NO^-, $n = 2$): (A) $[Ru^{II}(hedta)(^{14}NO^+)]\cdot xH_2O$; (B) $K[Ru^{II}(hedta)(^{14}NO\cdot)]\cdot xH_2O$; (C) $K_2[Ru^{II}(hedta)(^{15}NO^-)]\cdot xH_2O$.

located at 1426 and 1321 for $[Ru(bpy)_2(NO)(NO_2)]^{2+}$ [52b] but appear at lower frequency due to the higher reduced mass within $[Ru^{II}(hedta)(^{15}NO^+)(^{15}NO_2^-)]^-$. When excess $Na^{15}NO_2$ is present (3:1 Ru^{II}) in the precipitate, a third weak band is detected at 1107 cm^{-1} (Figure SF-5B in the Supporting Information). However, all other features at 3:1 were the same as those for the 2:1 preparation. The position of the two bands at 1370 and 1300 cm^{-1} indicate that the $^{15}NO_2^-$ ligand is attached through the N atom (nitro), not through O (nitrito).[60] The 2:1 complex compares well with the 1334 and 1285 cm^{-1} stretches for the nitro isomer of $[Ru(Cp)(NO_2)(PPh_3)_2]$[61] or the 1337 and 1292 cm^{-1} values for $[Ru(bpy)_2(CH_3CN)(NO_2)](PF_6)$.[62] When NO_2^- adopts the O-bound nitrito isomer, the $\nu_s(NO_2)$ band appears near 1130 cm^{-1} and $\nu_{as}(NO_2)$ near 1397 cm^{-1}.[60,63] The absence of this feature supports the thermodynamically stronger base site (N) as the mode of attachment to Ru^{II}. Furthermore, since the presence of $^{15}NO_2^-$ in $[Ru(hedta)(^{15}NO^+)(^{15}NO_2^-)]^-$ occurs with the displacement of a carboxylate donor, there is little reason for an O-bound NO_2^- to be able to compete as a σ-donor with the glycinato chelate, whereas the N-bound form can participate in both σ and π bonding with Ru^{II}.

The band at 1827 cm^{-1} is clearly that of the Ru^{II}-($^{15}NO^+$) chromophore. The related stretch in $[Ru^{II}(Cp)(NO^+)(PPh_3)_2]$-

(60) Nakamoto, K. *Infrared and Raman Spectra of Inorganic and Coordination Compounds*, 3rd ed.; Wiley: New York, 1978; pp 222−225.
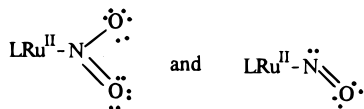(61) Szczepura, L. F.; Takeuchi, K. J. *Inorg. Chem.* **1990**, *29*, 1772.
(62) Adeyemi, S. A.; Miller, F. J.; Meyer, T. J. *Inorg. Chem.* **1972**, *11*, 994.
(63) Goodgame, D. M. L.; Hitchman, M. A.; Marshan, D. F.; Soutir, C. E. *J. Chem. Soc. A* **1969**, 2464.

(PF_6) appears at 1860 cm^{-1},[61] indicative of the $Ru(NO^+)$ formalism. The Ru^{II}−($^{14}NO^+$) complex was isolated separately as $[Ru^{II}(hedta)(^{14}NO^+)]\cdot xH_2O$ at 0.80:1.00 $Na^{14}NO_2$:$[Ru^{II}(hedta)(H_2O)]$. The solution was acidified by HCl to pH $\cong$ 1.5, followed by precipitation with acetone. The isolated solid had a pronounced $^{14}NO^+$ stretch at 1846 cm^{-1} (Figure 7A), higher than the 1827 cm^{-1} stretch of the $^{15}NO^+$ complex. A theoretical increase to 1851 cm^{-1} is calculated by application of the reduced mass ratio. The region between 1300 and 1400 cm^{-1} had much weaker stretches comparable to those of the $K[Ru^{II}(hedta)(H_2O)]$ complex. This indicates the absence of a coordinated nitro ligand at low pH as required by the equilibrium data presented previously in this paper.

Isolation of the same complex at higher pH of 7 or 9 did not yield a mixture of coordinated $^{14}NO^+$ and $^{14}NO_2^-$ complexes as anticipated by the same equilibrium. Rather, the Ru^{II}($^{14}NO^+$) species precipitated selectively, shifting the solution equilibrium. This prevented the isolation of a salt of $[Ru^{II}(hedta)(^{14}NO_2^-)]^{2-}$ free of its $[Ru^{II}(hedta)(^{14}NO^+)]$ partner.

When $K_2[Ru^{II}(hedta)(^{15}NO^-)]\cdot xH_2O$, isolated by Ar-induced evaporation of a sample shown to be 100% in the $^{15}NO^-$ form by ^{15}N NMR, was examined by the infrared technique, a strong

ν_{NO} band appeared at 1365 cm^{-1} that is not present in the [Ru(hedta)(H$_2$O)]$^-$ spectrum. The IR stretch for NO$^-$ ligands often appears near 1650 cm^{-1}.[64] However, this stretch occurs at 1390 cm^{-1} in the spectrum of Ni(Cp$^+$)(NO$^-$),[65] and since the atom arrangement is similar to that of a nitro complex as shown here, one mode could be very similar to ν_{as}(NO$_2$) which
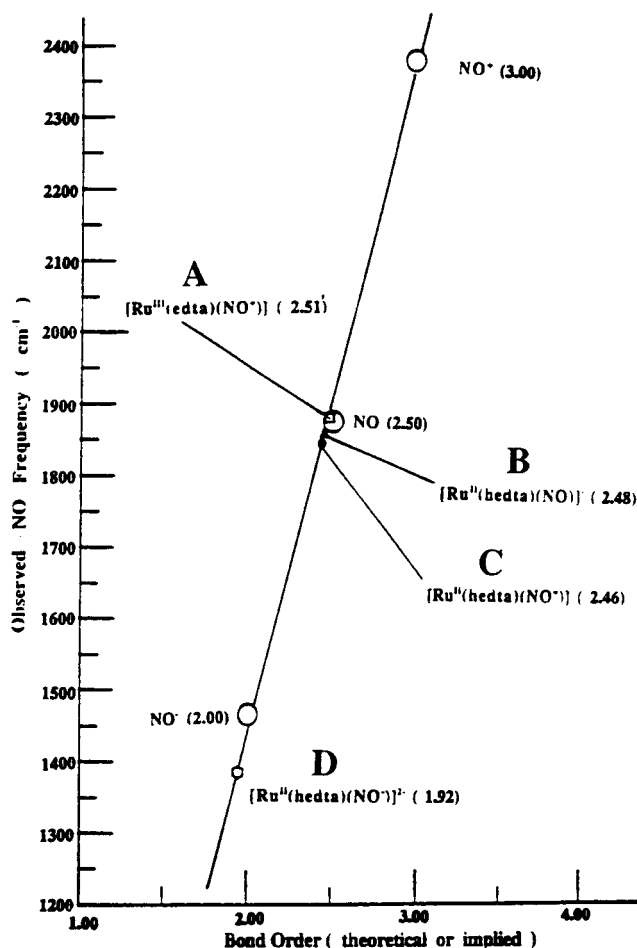
$$LRu^{II}-N\overset{\cdot\cdot\overset{\cdot\cdot}{O}\cdot}{\underset{\cdot\cdot\overset{\cdot\cdot}{O}\colon}{}} \quad \text{and} \quad LRu^{II}-\ddot{N}\overset{}{\underset{\cdot\cdot\overset{\cdot\cdot}{O}\cdot}{}}$$

as noted above appeared at 1370 cm^{-1} for Na[Ru^{II}(hedta)(^{15}NO$^+$)(^{15}NO$_2^-$)]·xH$_2$O. The ^{14}NO· complex K[Ru^{II}(hedta)(NO·)]·xH$_2$O was obtained by admission of ^{14}NO· to a solution of [Ru^{II}(hedta)(H$_2$O)]$^-$ over Zn/Hg. Introduction of ethanol to achieve a 50% ethanol solution was followed by chilling overnight. A solid crystalline product was filtered off, rinsed with acetone, and dried under N$_2$ in a glovebag. The KBr pellet of this product exhibited its ^{14}NO· stretch at 1858 cm^{-1} (Figure 7B). Reexamination of the spectrum of the ^{15}NO$^-$ complex revealed a trace impurity stretch at 1842 cm^{-1}, which would be consistent with the anticipated ^{15}NO· stretch of K[Ru^{II}-(hedta)(^{15}NO·)]·xH$_2$O present as a trace oxidation impurity of the more reduced K$_2$[Ru^{II}(hedta)(^{15}NO$^-$)]·xH$_2$O salt (Figure 7C). The NO stretches of the NO$^+$, NO·, and NO$^-$ complexes are summarized in the following series for their [Ru^{II}(hedta)] complexes:

	NO$^+$	NO·	NO$^-$
^{14}N	1846	1858	1383
^{15}N	1827	1842	1370

The NO stretching frequencies imply a slightly lower bond order for the NO$^+$ complex than for the NO· complex.[72] This can be

(64) (a) Botto, R. E.; Kolthammer, W. S.; Legzdins, P.; Roberts, J. D. *Inorg. Chem.* **1979**, *18*, 2049. (b) See refs 7 and 60.
(65) Crichton, O.; Rest, A. J. *J. Chem. Soc., Chem. Commun.* **1973**, 407.
(66) Gratzel, M.; Taniguchi, S.; Henglin, A. *Ber. Bunsen.-Ges. Phys. Chem.* **1970**, *74*, 1003.
(67) (a) Matsubara, T.; Creutz, C. *J. Am. Chem. Soc.* **1978**, *100*, 6255. (b) Matsubara, T.; Creutz, C. *Inorg. Chem.* **1979**, *18*, 1956. (c) Zang, V.; Kotowski, M.; van Eldik, R. *Inorg. Chem.* **1988**, *27*, 3279. (d) Zang, V.; van Eldik, R. *Inorg. Chem.* **1990**, *29*, 1705.
(68) Farrell, N.; Dolphin, D.; James, B. R. *J. Am. Chem. Soc.* **1978**, *100*, 324.
(69) Wink, D. A.; Grisham, M. B.; Mitchell, J. B.; Ford, P. C. In *Methods in Enzymology*; Packer, L., Ed.; Academic Press: New York, 1996; Vol. 268, pp 13−31.
(70) Taqui Khan, M. M.; Venkatasubramanian, K.; Shirin, Z.; Bhadbhade, M. M. *J. Chem. Soc., Dalton Trans.* **1992**, 1031.
(71) Ward, M. A.; Shepherd, R. E. *Inorg. Chim. Acta*, in press.
(72) A plot of ν_{NO} vs bond order for NO$^+$ (3.00), NO· (2.50), and NO$^-$ (2.00) is linear. See Figure 8. The observed ν_{NO} values for [Ru^{III}-(edta)(NO$^+$)], [Ru^{II}(hedta)(NO·)]$^-$, [Ru^{II}(hedta)(NO$^+$)], and [Ru^{II}-(hedta)(NO$^-$)]$^{2-}$ are consistent with respective bond orders of 2.51, 2.48, 2.46, and 1.92. Arguments that no relationship exists among various complexes for ν_{NO}, bond angle, and NO$^+$ assignment have been noted elsewhere.[5−7] But within a constant ligand set, such comparisons are believed to be more valid.[6,7] Thus comparisons among the specified complexes have been made here. As a check of the validity of these comparisons, a plot of the observed NO distance for standard compounds was shown to be linear in bond order (see Figure SF-6). Then the implied NO bond order based on the known 1.141 Å bond distance for [Ru^{III}(edta)(NO$^+$)] was shown to be 2.58 based on the standard compounds. This agrees reasonably well with the 2.51 value determined by the frequency method using the linearity of the ν_{NO} vs bond order plot in Figure 8. Also, the data of Figure 8 support the intuitive idea that back-donation is greater for Ru^{II} than for Ru^{III}, but Ru^{II} also withdraws σ density less well. Thus both Ru^{III} and Ru^{II} lower the NO$^+$ bond order, but because of different factors.
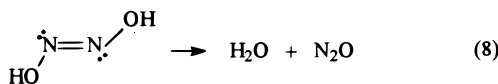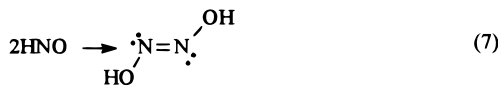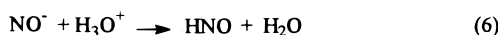
Figure 8. Implied NO bond orders for [Ru(edta)] and [Ru(hedta)] complexes of NO$^+$, NO, or NO$^-$ based on NO infrared frequency data. The theoretical line was established by free NO$^+$, NO, and NO$^-$ literature frequency data.[7,60] The bond orders of the ruthenium "NO" complex are given in parentheses; note the reasonable agreement for the [Ru^{III}(edta)(NO$^+$)] complex with that implied by X-ray methods ($\nu_{NO} = 1880$ cm^{-1}) for [Ru^{III}(edta)(NO$^+$)];[70] other ν_{NO} values were taken from this work. Complexes: (A) [Ru^{III}(edta)(NO$^+$)]; (B) [Ru^{II}(hedta)-(NO)]$^-$; (C) [Ru^{II}(hedta)(NO$^+$)]; (D) [Ru(hedta)(NO$^-$)]$^{2-}$.

explained by the linear coordination for NO$^+$ vs bent coordination for NO·. Back-donation will be greater from Ru^{II} to the NO$^+$ ligand by virtue of its positive charge and no antibonding electrons in the π^* orbitals, compared to no charge and one repulsive electron for NO·. When the orbital overlap is good for the Ru^{II}−NO$^+$ chromophore, donation of dπ density increases the σ donation from NO$^+$. This depletes the σ-bonding density between N and O as well as reducing the net π-bonding electron density. The poorer overlap and angular contact required for NO· as a ligand result in much less transfer of dπ density from Ru^{II} to NO· which already has one full π^* electron. Additional back-donation is disfavored relative to NO$^+$, and the lower formal charge left at the Ru^{II} center has a less polarizing effect on the σ-donated pair from NO· than an effective Ru^{III}-like center has on coordinated NO$^+$. The outcome is that the bond order for coordinated NO· is slightly greater than that for NO$^+$, both being near 2.48 (see Figure 8). Taqui Khan and co-workers have isolated [Ru^{III}(edta)(NO$^+$)], which has its ν_{NO^+} at 1880 cm^{-1}.[70] Their results are consistent with ours in that the Ru^{III}(NO$^+$) chromophore should have poorer back-donation

(73) (a) Swinehart, J. M.; Rock, D. A. *Inorg. Chem.* **1966**, *5*, 578. (b) Swinehart, J. M. *Coord. Chem. Rev.* **1967**, *2*, 385.
(74) Khanna, R.; Brown, C. W.; Jones, L. H. *Inorg. Chem.* **1969**, *8*, 2195.

and a higher ν_{NO^+} than those for the analogous $Ru^{II}(NO^+)$ species. Both $[Ru^{III}(edta)(NO^+)]$ and $[Ru^{II}(hedta)(NO^+)]$ have cis-equatorial geometries with pendant carboxylate and alcohol functionalities, respectively. The higher ν_{NO^+} of 1880 cm^{-1} for Ru(III) is indeed greater than 1846 cm^{-1} for Ru(II) in the anticipated order, substantiating lesser back-donation in $[Ru^{III}-(edta)(NO^+)]$ than in $[Ru^{II}(hedta)(NO^+)]$. When the NO ligand is fully reduced to NO$^-$, back-donation from Ru^{II} is decreased even more. The back-bonding appears to be greater than zero, given the lower ν_{NO^-} stretch for $[Ru^{II}(hedta)(NO^-)]^{2-}$ compared to 1650 cm^{-1} observed for other complexes and 1470 cm^{-1} for free NO$^-$.[64]

Stability of the NO$^-$ Complex. Acidifying a sample of $[Ru(hedta)(^{15}NO^-)]^{2-}$, which exhibited only the ^{15}N NMR pair of resonances at 609 and 607 ppm at pD $\sim$ 6, led to a pD of ca. 2 without loss of the 609/607 resonance pair. Thus, coordination to $[Ru^{II}(hedta)]^-$ prevents the rapid conversion of NO$^-$ to N$_2$O, which is the known sequence of free NO$^-$ in aqueous acidic solution (eqs 6–8). The normal pK_a of HNO is

$$NO^- + H_3O^+ \longrightarrow HNO + H_2O \qquad (6)$$

$$2HNO \longrightarrow \overset{\cdot\cdot}{N} = N \overset{OH}{\underset{\cdot\cdot}{\overset{\cdot\cdot}{}}} \qquad (7)$$
$$\overset{HO}{}$$

$$\overset{\cdot\cdot}{N} = N \overset{OH}{\underset{\cdot\cdot}{}} \longrightarrow H_2O + N_2O \qquad (8)$$
$$\overset{HO}{}$$

4.7.[66] Assuming the influence of $[Ru^{II}(hedta)]^-$ on the acidity of coordinated HX ligands is similar to the influence on coordinated HONO as discussed in a former section, the pK_a of coordinated HNO would be ca. 1.0 or below. Thus the observation that $[Ru(hedta)(NO^-)]^{2-}$ persists at pD $\sim$ 2.0 is in concert with this estimate. Additionally, protonation of coordinated NO$^-$ removes a lone pair required to achieve dimerization along the pathway to N$_2$O. Therefore, the N$_2$O production in Meyer's study[26] of the electrochemical catalytic reduction of NO$_2^-$ must occur via an efficient pathway involving dissociation of NO$^-$ from an $[Ru^{II}(Hedta)(NO^-)]^{2-}$ intermediate. The reason for a lower affinity for a protonated edta complex vs the $[Ru^{II}(hedta)(NO^-)]^{2-}$ of this report is not obvious. However, the pendant carboxylate functionality of the $[Ru^{II}-(edta)]^{2-}$ system is known to labilize the substitution of ligands in the first coordination sphere, whereas pendant alcohol functionalities do not.[67] This feature was seen to induce fluxional behavior in the pyrimidine adjacent to a pendant carboxylate, yet keeping stereochemically rigid behavior for a pyrimidine adjacent to the alcohol arm in the $[Ru^{II}(hedta)(pym)_2]^-$ complex.[43] This complex has the structure shown here with the starred pyrimidine executing 1,3-metallotropic shifts.[43]
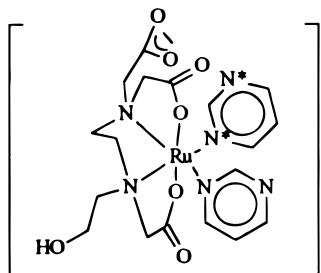
The "on–off" attack of a carboxylato group could help labilize the cis-bound HNO ligand within an $[Ru^{II}(Hedta)(HNO)]^-$ complex, leading to N$_2$O formation via eqs 6–8. The structurally

Chart 1

Starting Relative d Energies

Resultant MO Patterns
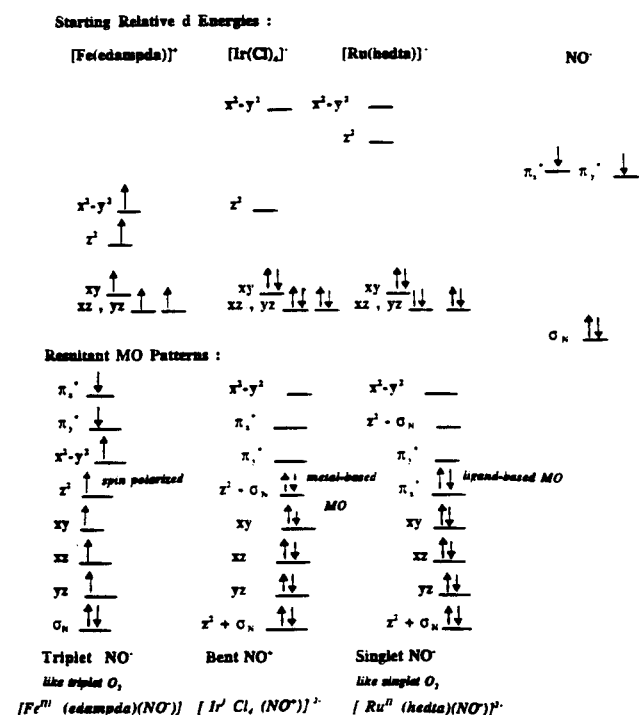
similar $[Ru^{II}(hedta)(NO^-)]^{2-}$ complex would be protected since all carboxylates are coordinated in either the cis-equatorial or trans-equatorial isomer whereas for the edta complex the pendant arm position is occupied by a more nucleophilic carboxylate group:

cis-equatorial isomer   trans-equatorial isomer
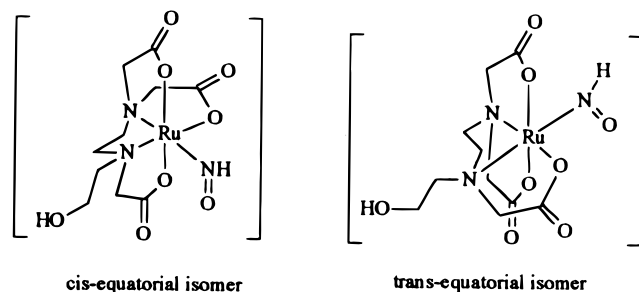
MO Treatment for Coordinated NO Moieties. There have been numerous MO treatments for coordinated metal nitrosyls in previous papers and reviews.[32–35] It is worthwhile to emphasize that differences which are observed in the nature of the coordinated NO ligand as NO$^+$, NO$^-$ triplet, NO$^-$ singlet, and NO$\cdot$ are predominantly a function of the relative energy of the $d_{x^2-y^2}$ and d_{z^2} orbitals in comparison with the π_x^* and π_y^* levels of NO and NO$^-$. In Chart 1 the situations for high-spin Fe^{III}, low-spin Ir^{III}, and low-spin Ru^{II} are compared. The Fe^{III} orbitals reside below the π^* levels of NO$^-$ and above the σ lone pair on N of NO$^-$. The Ir^{III} situation in a five-coordinate complex places $d_{x^2-y^2}$ above the π^* levels of NO, but d_{z^2} below. With Ru^{II}, both $d_{x^2-y^2}$ and d_{z^2} lie above the π_x^* and π_y^* NO$^-$ levels. In the cases of Ir^{III} and Ru^{II}, σ_N of NO can mix with d_{z^2} favorably. Due to the difference in the relative placement of d_{z^2} for Ir^{III} and Ru^{II}, the antibonding combination $d_{z^2}-\sigma_N$ resides below the π^* levels of coordinated NO for Ir^{III}, which are also split by the complex's symmetry into nondegenerate π^* levels. By contrast, the same $d_{z^2}-\sigma_N$ MO combination resides energetically above both π^* levels parented by NO$^-$ in the Ru^{II} complex. For Fe^{III}, the situation places both π_x^* and π_y^* above all the

metal center's d orbitals, which as a group are above σ_N of NO.

With only a spin-polarization interaction for Fe^{III} and NO$^-$, the resultant filling produces a triplet NO$^-$, analogous to triplet O$_2$; spin-polarization accounts for the net spin state of $S = {}^3/_2$.[19-21] There is no net change in oxidation states as constructed from HS Fe^{III} plus NO$^-$ in Chart 1. In reality, such species are generated by one-electron transfer between HS Fe^{II} and NO•, forming the {Fe^{III}—triplet NO$^-$} species.[71]

When d$_{z^2}$ resides below the π^* levels of NO$^-$, the resultant filling of orbitals populates the antibonding d$_{z^2}$–σ_N combination MO. Since this has a significant metal orbital contribution, the electron pair generated from a d^6 metal center plus NO$^-$ places a large formal electron density component on the metal center. Hence, the complex is formally reduced to d^8 by the two electrons that were available from NO$^-$. The NO ligand is formally NO$^+$, but it is bent for the M—NO bond because of the symmetry difference for π_x^* and π_y^* and the antibonding nature of d$_{z^2}$–σ_N. Thus an Ir^{III} plus NO$^-$, Co^{III} plus NO$^-$, or other strong-field complexes in need of only five ligands to produce 16e$^-$, five-coordinate species become M^I(d^8)–*bent NO$^+$* systems as explained previously.[13]

The case of Ru^{II} wherein a low-spin d^6 center has both d$_{x^2-y^2}$ and d$_{z^2}$ levels above the π^*(NO) orbitals has not been described as for the Ir^{III}—NO$^-$ $\leftrightarrow$ Ir^I—NO$^+$ resonance situation that ultimately applies to most organometallic nitrosyl complexes and, hence, which has received the most theoretical attention.[13,32-35] The outcome for LS Ru^{II} is to place the two electrons donated by NO$^-$(g) into a nondegenerate π^* ligand MO. Hence, the oxidation states of the ruthenium center and NO ligand remain Ru(II) and NO$^-$ as before their combination. But the removal of degeneracy of the π_x^* and π_y^* ligand orbitals and the localization of the electron in π_x^* produces a bent M—NO bond. The coordinated NO$^-$ is a singlet NO$^-$, analogous to singlet O$_2$. No stable [Ru^{II}(hedta)(dioxygen)] complex is known. However, a reversible Ru^{II} dioxygen complex of Ru(TPP) and Ru(OEP) (TPP = tetraphenylporphyrin; OEP = octaethylporphyrin) in pyrrole at 20 °C was reported by Farrell, Dolphin, and James.[68] There were no EPR signals ascribable to a Ru^{III}—O$_2{}^-$ electronic arrangement. Hence, their data could be interpreted as supporting a Ru^{II}—O$_2$ singlet complex although no statement was made by the authors claiming this as the correct electronic arrangement.

Conclusions

Evidence has been provided for distinctly different [Ru^{II}-(hedta)L]$^{n-1}$ complexes of L—NO$^+$, NO•, and NO$^-$. These differ according to infrared spectroscopy with ν_{NO} values of 1846, 1858, and 1383 cm^{-1}, respectively, for ^{14}N. The NO$^+$ species exhibits an ^{15}N NMR chemical shift at 249.6 ppm vs formamide. The NO$^+$ complex exists as only one stereochemical isomer,

the cis-equatorial [Ru^{II}(hedta)(NO$^+$)] complex. The NO$^-$ complex has its ^{15}N NMR chemical shift at 609.4 and 607.4 ppm for two isomers of [Ru(hedta)(NO$^-$)]$^{2-}$ which are the cis-equatorial and trans-equatorial isomers. Both are singlet NO$^-$ complexes which are protected against rapid proton-induced reactions which form N$_2$O from the dissociated HNO ligand. The one-electron reduction potentials for [Ru(hedta)L]$^{1-n}$ species are -0.37 V for the NO$^-$/NO• complex couple, -0.10 V for the NO•/NO$^+$ couple, and a metal-centered Ru^{II}(NO$^+$)/Ru^{III}(NO$^+$) wave at $+0.98$ V (in acidic solution).

The reaction [LRu^{II}(NO$^+$)]^m + 2OH$^-$ $\rightleftharpoons$ [LRu^{II}(NO$_2{}^-$)]$^{m-2}$ + H$_2$O has been shown to have an equilibrium constant, $K_{NO_2^-}$, that responds in a predictable fashion depending on the outer-sphere preassociation constant for one hydroxide. This is followed by a proton transfer to the second hydroxide. The log-($K_{NO_2^-}$) value is linear in $-z_1z_2$ of the ion pair as long as the secondary ligand set does not enter into highly specific H-bonding with water, as is the case for tetraammine complexes. The magnitude of $K_{NO_2^-}$ is such that 50% of the [Ru^{II}(hedta)] complex is present in the NO$^+$ form and 50% as the nitro complex at pH = 7.42.

The [Ru(hedta)(NO$^+$)] complex shows substantial back-donation which lowers its ν_{NO} relative to more withdrawing ligand sets such as (CN$^-$)$_5$ or polypyridyl donors. As a consequence, there is substantial Ru^{III}(NO) and Ru^{IV}(NO$^-$) character even though the ligand is clearly NO$^+$ according to its ^{15}N NMR shift.

The MO results show that it is unlikely that NO$^-$ is transported in biochemical cells as an NO$^-$ singlet complex, as there are few metallo species having sufficiently strong ligand fields or having second transition series metal centers available. It is already known that metmyoglobin rapidly traps NO$^-$, but only via NO$^-$ reduction of the Cu^{II} center of superoxide dismutase, followed by NO trapping with metmyoglobin.[22,23,69] There may be a physiological advantage to [Ru^{II}(hedta)(NO$^+$)] as an NO$^+$ transport agent. Its lower charge may make passage through the kidney barrier more facile than for the edta^{4-} complex. Related ligands deserve further testing to determine the best ruthenium-based antisepsis agents. To these ends, related ligand series of mixed carboxylate and pyridyl donor sets are under study in our laboratories.[71]

Supporting Information Available: Figures SF-1–SF-6, showing additional differential pulse voltammograms, NMR spectra, IR spectra, and isomer distribution and NO bond order plots. This material is available free of charge on the Internet at http://pubs.acs.org.

IC980868E